Advances in Machinery, Materials Science and Engineering Application
M. Chen et al. (Eds.)

doi:10.3233/ATDE220444

Using the -Bdot Algorithm to Reduce the Angular Velocity of Rotation for the Aist Small Spacecraft Pilot Model

Andrey Sedelnikov [a,1], Denis Orlov [a], Ekaterina Khnyryova [a], Alexandra Nikolaeva [a] and Maria Bratkova [a]
[a] *Institute of Aerospace Engineering of Samara National Research University, 34, Moskovskoye Shosse, Samara, 443086, Russia*

Abstract. This article considers the issues of reducing the angular velocity of rotation for a small spacecraft operated in uncontrolled flight. A mathematical model based on Euler's dynamic equations in the main coupled coordinate system of a small spacecraft has been constructed. The transition of the inertia tensor of the Aist small spacecraft pilot model from the bench coordinate system to the main connected coordinate system was performed. A study and evaluation of the significance of various disturbing factors in modeling the rotational motion of a small spacecraft around the center of mass has been carried out. At the same time, gravitational, aerodynamic and magnetic disturbing factors are considered. The application of the -Bdot algorithm by magnetic executive bodies to reduce the angular velocity has been studied. Results are obtained demonstrating the effectiveness of the -Bdot algorithm application on the example of the Aist small spacecraft pilot model. The results of the presented work can be used in the development of effective algorithms for controlling the movement of a small spacecraft around the center of mass in order to reduce the angular velocity of its rotational motion.

Keywords. Small spacecraft, reducing the angular velocity, magnetic executive bodies, -Bdot algorithm

1. Introduction

When flying a small spacecraft without control, it is necessary to reduce the value of the rotation speed relative to the center of rotation. Studies [1–3] show the relationship between the angular velocity of a small spacecraft rotation and the quality of receiving and transmitting telemetric data. If we are talking about small spacecraft for the Earth remote sensing [4–6] or for specialized technological purposes [7–9], then the values of the angular velocity of rotation in this case should be significantly limited for the successful fulfillment of target tasks.

The task of maintaining the target range for the angular velocity of rotational motion is solved by various methods and executive bodies, depending on the spacecraft purpose. Thus, restrictions on the accuracy of orientation and stabilization of the earth observation spacecraft lead to the fact that in order to perform target tasks with a given quality, the

[1] Andrey Sedelnikov, Corresponding author, Institute of Aerospace Engineering of Samara National Research University, 34, Moskovskoye Shosse, Samara, 443086, Russia; E-mail: axe_backdraft@inbox.ru.

motion control system of the Aist-2D small spacecraft provides the value of the angular velocity of rotation not higher than 0.05 deg/s [10].

Despite the fact that specialized vibration protection devices are often used to implement experiments and studies that impose restrictions on the gravity change [11–15], the spacecraft rotational motion should not create unacceptably high microaccelerations [16, 17].

Thus, reducing the angular velocity of the rotational motion of a small spacecraft is an important and urgent modern task. The paper considers the use of the well-known -Bdot algorithm [18, 19] to reduce the angular velocity of rotation for a small spacecraft without large elastic elements. It is assumed that the spacecraft is operated in non-orientated flight. Magnetic executive bodies are considered as executive bodies for reducing the angular velocity.

2. Mathematical Model for a Small Spacecraft Rotational Motion

As a basic small spacecraft for the computational experiment, a pilot model of the Aist small spacecraft was chosen [1, 3, 6, 10]. The launch of this small spacecraft (figure 1) was carried out on December 28, 2013 by separation from the Volga upper stage, placed into a near-circular orbit with a height of 625 km and an inclination of 82.40 from the Plesetsk cosmodrome by the Soyuz-2-1v launch vehicle. The mass of this device is 39 kg, including 11 kg of equipment for scientific research.

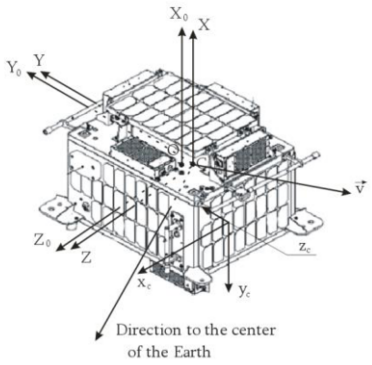

Figure 1. Pilot model of the Aist small spacecraft and used coordinate systems: $OX_0Y_0Z_0$ is the bench coordinate system in which the components of the small spacecraft inertia tensor were determined (point O is the geometric center of a small spacecraft); *CXYZ* is the main body axis coordinate system with the origin at the center of mass (point C) of a small spacecraft; $x_cy_cz_c$ is the structural coordinate system of magnetometer № 2 (this coordinate system is left) (cited of [20]).

The rotational motion of a small spacecraft will be considered in the main body axis coordinate system (figure 1). In [3], the Euler dynamic equations were obtained in the main body axis coordinate system (*CXYZ*):

$$\begin{cases} \varepsilon_x = \dfrac{(M_{mx} + M_{gx} + M_{ax} + M_{cx})}{I_x} - \dfrac{I_z - I_y}{I_x}\omega_y\omega_x; \\ \varepsilon_y = \dfrac{(M_{my} + M_{gy} + M_{ay} + M_{cy})}{I_y} - \dfrac{I_x - I_z}{I_y}\omega_x\omega_y; \\ \varepsilon_z = \dfrac{(M_{mz} + M_{gz} + M_{az} + M_{cz})}{I_z} - \dfrac{I_y - I_x}{I_z}\omega_x\omega_y, \end{cases} \quad (1)$$

where I_x, I_y, I_z are diagonal tensor components in main body axes; $\vec{\varepsilon}\left(\varepsilon_x, \varepsilon_y, \varepsilon_z\right)$ and $\vec{\omega}\left(\omega_x, \omega_y, \omega_z\right)$ are vectors of angular acceleration and angular velocity and their projections in the main body axis coordinate system, respectively; $\vec{M}_m\left(M_{mx}, M_{my}, M_{mz}\right)$, $\vec{M}_g\left(M_{gx}, M_{gy}, M_{gz}\right)$, $\vec{M}_a\left(M_{ax}, M_{ay}, M_{az}\right)$ and $\vec{M}_c\left(M_{cx}, M_{cy}, M_{cz}\right)$ are vectors of magnetic, gravitational, aerodynamic and control moments and their projections in the main body axis coordinate system, respectively.

Let us estimate the significance for each of the disturbing influences included in equation (1). During ground tests of Aist small spacecraft pilot model, the axial and centrifugal moments of inertia in the axes of the test bench were experimentally established *($OX_0Y_0Z_0$)* [10, 20]:

$$\hat{I} = \begin{pmatrix} 1.7 & -1.0 & -0.8 \\ -1.0 & 1.2 & -1.1 \\ -0.8 & -1.1 & 1.5 \end{pmatrix} \quad (2)$$

Conversation to the main body axes coordinate system was carried out using the following formula:

$$\det\left(\hat{I} - \lambda E\right) = 0 \quad (3)$$

where $\lambda(\lambda_1, \lambda_2, \lambda_3)$ are eigenvector components; E is the identity matrix.

Application (3) to (2) gives the values for the inertia tensor components of Aist small spacecraft pilot model in the main body axes coordinate system (*CXYZ*):

$$\hat{I} = \begin{pmatrix} 2.4 & 0 & 0 \\ 0 & 1.7 & 0 \\ 0 & 0 & 2.1 \end{pmatrix} \quad (4)$$

Let us estimate the value of the gravitational perturbing moment by the formula [1, 20]:

$$\left|\vec{M}_g\right| = \left|\frac{3\mu}{r^3}\vec{e}_r \times \left(\hat{I}\cdot\vec{e}_r\right)\right| \tag{5}$$

where μ is the gravitational parameter of the Earth; r is the orbit radius Aist small spacecraft pilot model; $\vec{e}_r$ is the unit vector of the direction to the Earth's center, which is shown in figure 1.

In the main body axes coordinate system, the gravitational perturbing moment will be equal to zero, since the gravitational force passes through the center of mass and crosses all coordinate axes. This is also seen from expression (5). The vectors $\vec{e}_r$ and $\hat{I}\cdot\vec{e}_r$ are collinear, given the structure of the inertia tensor in the main axes (4). Therefore, their cross product is zero.

In [20], an estimate of the average aerodynamic force acting on Aist small spacecraft pilot model is given. It is approximately equal to $1{,}2\cdot10^{-6}$ *N*. Let us refine it by using the data for another similar spacecraft - the flight model of the Aist small spacecraft [5, 10]. The orbital parameters of the pilot model and flight model of the Aist small spacecraft are given in table 1 [10].

Table 1. Orbital parameters of the pilot model and flight model of the Aist small spacecraft.

Parameter	Flight model		Pilot model	
	04/21/2013	**08/23/2016**	**12/28/2013**	**08/23/2016**
Inclination *i*, °	64.877	64.874	82.424	82.419
Ellipticity *e*	0.001386	0.001427	0.002017	0.001889
Pericenter altitude h_p, km	584.055	571.832	633.598	626.418
Apocenter altitude h_a, km	564.801	552.048	605.399	600.033

Table 1 shows that the orbits of small spacecraft are weakly elliptical. However, to simplify calculations, we will consider them near-circular with radii of:

$$R = \frac{1}{2}\left(h_p + h_a\right). \tag{6}$$

We believe that the angular velocity of the rotational motion of small spacecraft did not change significantly between the measurements. Basing on this proposal, we conclude that the kinetic energy of small spacecraft has changed due to a decrease in altitude and aerodynamic braking:

$$\Delta T = A\left(\vec{G}\right) + A\left(\vec{F}_{aer}\right). \tag{7}$$

Wherein:

$$\Delta T = f\frac{m_s M}{2}\left(\frac{1}{R_1}-\frac{1}{R_0}\right), \tag{8}$$

where f is the gravitation constant; m_s and M are the masses of the small spacecraft and the Earth, respectively; R_0 and R_1 are radii of near-circular orbits calculated by formula (6), respectively.

The value for the work of the gravitational force $A\left(\vec{G}\right)$ is related to the change in the potential energy of a small spacecraft as a result of a decrease in the orbit radius:

$$A\left(\vec{G}\right) = -\Delta E_p = m_s g\left(R_0 - R_1\right). \tag{9}$$

Then, using formula (7), we can estimate the work of the aerodynamic drag force $A\left(\vec{F}_{aer}\right)$. Next, we can estimate the average value for the force, knowing which trajectory the small spacecraft traveled during the measurement time:

$$\bar{F}_{aer} = \frac{A\left(\vec{F}_{aer}\right)}{s}. \tag{10}$$

The results of the assessments carried out are presented in table 2.

Table 2. Orbital parameters of the pilot model and flight model of the Aist small spacecraft.

Parameter	Flight model	Pilot model
ΔT, *MJ*	2.024	1.003
$A\left(\vec{G}\right)$, *MJ*	4.111	2.065
$A\left(\vec{F}_{aer}\right)$, *MJ*	-2.087	-1.062
Number of revolution	18300	14440
s, km	$7.979\cdot10^8$	$6.339\cdot10^8$
$\vec{F}_{aer}$, *μN*	2.615	1.676

The difference in estimates $\vec{F}_{aer}$ can be explained by different altitudes of the operation orbit of the pilot model and flight model of the Aist small spacecraft. Since the flight model was in a lower orbit compared to the pilot model, it experienced more aerodynamic drag.

The moment from $\vec{F}_{aer}$ relative to the center of mass for a small spacecraft depends on the components of the radius vector of the point O in the main body axes coordinate system *CXYZ* (figure 1). Strictly speaking, as the small spacecraft rotates, this distance

changes. Taking the average value equal to 3 cm, we get: $\left|\vec{M}_a\right| = \bar{M}_C\left(\bar{F}_{aer}\right) \approx 5 \cdot 10^{-8}\ N \cdot m.$

When estimating the maximum value of the magnetic perturbing moment, we use the well-known formula [6, 18, 20]:

$$\vec{M}_m = \sum_{j=1}^{n} \vec{p}_j \times \vec{B}, \tag{11}$$

where $\vec{p}_j$ is the magnetic moment of the j-th circuit with current; n is the number of circuits with current; $\vec{B}$ is the induction vector of the Earth's magnetic field.

We will make two estimates: during the operation of magnetic executive bodies and during the period when they do not work. In the first case, we will assume that the magnetic executive bodies create the maximum disturbing moment. According to the technical data sheet, the magnetic moment of the current for the magnetic executive bodies was 0.5 $A \cdot м^2$ for each control channel [20]. Assuming that the maximum value of $\vec{B}_{\max} = 60\ \mu T,$ we will have:

$$\left|\vec{M}_c\right|_{\max} = \left|\vec{p}_c\right|_{\max} \left|\vec{B}_{\max}\right| \approx 5 \cdot 10^{-5}\ N \cdot m, \tag{12}$$

where $\left|\vec{p}_c\right|_{\max} = \sqrt{0.5^2 + 0.5^2 + 0.5^2} \approx 0.866\ A \cdot m^2$ is the maximum magnetic moment of all three magnetic executive bodies operating at the maximum value of the current in the circuits.

During the period when the magnetic executive bodies do not work, we will consider the battery charging circuit as the main disturbing factor. We will calculate the magnetic moment of the current by the formula [6, 18, 20]:

$$\vec{p} = i S \vec{n}, \tag{13}$$

where $\vec{n}$ is the unit normal vector to the circuit area S.

Taking into account the maximum dimensions of the Aist small spacecraft pilot model (400x500x600 mm) [10], we have the maximum area of the circuit with current: $S_{\max} = 0.5 \cdot 0.6 = 0.3 m^2$. When the normal vector and the Sun direction vector coincide, we get the largest value of the current strength on the one panel, which is $i_{\max} = 1A$ [6, 21]. Then the use of formulas (11) and (13) gives the following estimate:

$$\left|\vec{M}_m\right|_{\max} = \left|\vec{p}_m\right|_{\max} \left|\vec{B}_{\max}\right| = 1.8 \cdot 10^{-5}\ N \cdot m. \tag{14}$$

Estimate (14) is slightly higher than the estimate made in [20] ($\left|\vec{M}_m\right|_{\max} = 1.5 \cdot 10^{-5}\ N \cdot m$), due to the fact that in [20] the degradation of photoconverters at the time of measurements was taken into account.

Taking into account the estimates made, the equations of rotational motion (1) can be rewritten in the following form, leaving the most significant perturbing factors:

$$\begin{cases} \varepsilon_x = \dfrac{\left(M_{mx} + M_{cx}\right)}{I_x} - \dfrac{I_z - I_y}{I_x}\omega_y\omega_z; \\ \varepsilon_y = \dfrac{\left(M_{my} + M_{cy}\right)}{I_y} - \dfrac{I_x - I_z}{I_y}\omega_x\omega_y; \\ \varepsilon_z = \dfrac{\left(M_{mz} + M_{cz}\right)}{I_z} - \dfrac{I_y - I_x}{I_z}\omega_x\omega_y. \end{cases} \quad (15)$$

3. Data for Numerical Simulation

For numerical simulation, we use a pilot model of the Aist small spacecraft (figure 1). Its inertia tensor in the main axes has the form (4), the orbit parameters are given in table 1. Numerical simulation will use measurements of the Earth's magnetic field induction vector using two three-component magnetometers (figure 2 [22, 23]).

Figure 2. Appearance of a three-component magnetometer installed on board a pilot model of the Aist small spacecraft.

An example of these measurements is shown in figure 3. For their processing, the moving average method was used [24, 25].

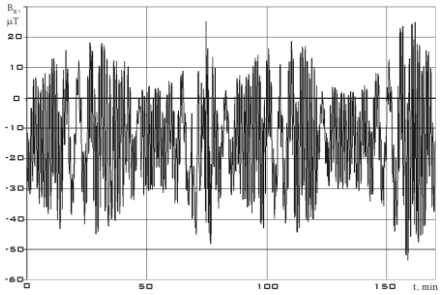

Figure 3. Example of magnetometer measurement data from 01/14/2014.

When estimating the control torque $\vec{M}_c$, data were used on the current in the power supply system of the Aist small spacecraft pilot model (figure 4 [20, 26]), as well as the current supplied to the executive bodies of magnetic type (figure 5 [20, 27]).

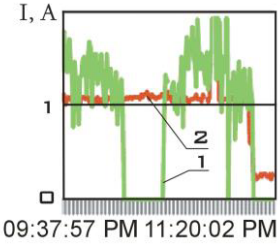

Figure 4. Current in the power supply system of the Aist small spacecraft pilot model from 03/25/2014: 1 is in the battery charging circuit; 2 is in the power consumption circuit of scientific equipment.

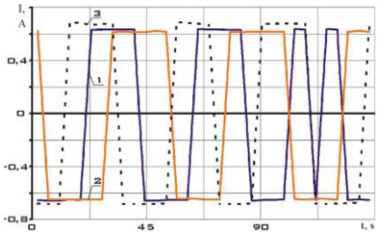

Figure 5. The dynamics of the current strength in the magnetic executive bodies, implemented on the Aist small spacecraft pilot model.

4. Numerical Simulation Results

Using equation (15), we will estimate the motion parameter of the Aist small spacecraft pilot model around the center of rotation without the control moment and with the control moment $\vec{M}_c$. As a control algorithm, we will use the well-known -Bdot algorithm [18, 28-30]:

$$\vec{M}_c = -\frac{k_\omega}{|\vec{B}|}\frac{d\vec{B}}{dt}, \tag{16}$$

where k_ω is the constant coefficient, which depends on the characteristics of the magnetic executive bodies.

For the measurement data of January 11, 2014 [1, 24, 31], the dependences of the disturbing moments without control and with control are obtained, shown in figure 6. The coefficient k_ω was taken equal to 10.

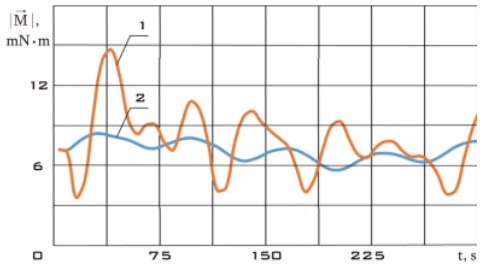

Figure 6. Dependence of the disturbing moment on time according to measurements on the Aist small spacecraft pilot model dated 01/11/2014: 1 is without control; 2 is with control using -Bdot algorithm.

The rotational motion parameters corresponding to disturbances (figure 6) are shown in figures 7 (angular acceleration) and 8 (angular velocity).

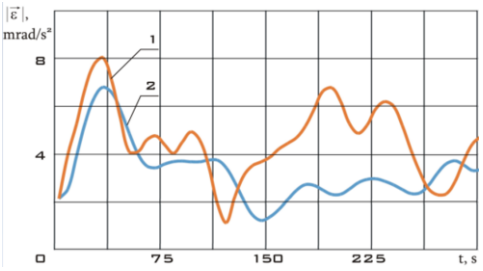

Figure 7. The dependence of the angular acceleration for the rotational motion of the Aist small spacecraft pilot model on time, corresponding to the disturbances shown in figure 6: 1 is without control; 2 is with control using -Bdot algorithm.

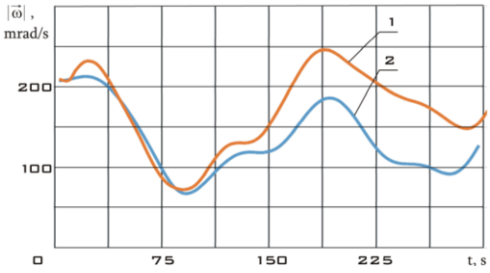

Figure 8. The dependence of the angular velocity for the rotational motion of the Aist small spacecraft pilot model on time, corresponding to the acceleration shown in figure 7: 1 is without control; 2 is with control using -Bdot algorithm.

Figure 8 confirms that the use of the "-Bdot" control algorithm makes it possible to reduce the rotation speed relative to the center of rotation of a small spacecraft to the required level.

5. Conclusions

Thus, the work is devoted to modeling the usage of the "-Bdot" algorithm to reduce the angular velocity of the rotational motion of the Aist small spacecraft pilot model. The results of [1, 3, 6, 18, 20, 30], which indicate the efficiency of using such control

algorithms, have been confirmed. However, when using the "-Bdot" algorithm, it is necessary to accurately estimate the components of the magnetic field induction vector of our planet [19]. For this algorithm, it is necessary to study the operation of measuring instruments in conditions of dense location and under the influence of the equipment operation to ensure the functioning of the spacecraft, including the executive bodies, the target equipment of the spacecraft [32]. Ignoring this influence can lead to incorrect operation of the algorithm and, ultimately, to an increase in the rotation speed relative to the center of rotation. This is indicated in the works [1, 3, 13, 20, 24].

Conflicts of Interest

The authors declare no conflicts of interest.

References

[1] Belousova DA, Serdakova VV. Modeling the temperature shock of elastic elements using a one-dimensional model of thermal conductivity. International Journal of Modeling, Simulation and Scientific Computing. 2020; 11(6) 2050060.
[2] Qu Z, Zhang G, Meng Z, Xu K, Xu R, Di J. Simulation of a flexible spacecraft motion to evaluate microaccelerations. Aerospace. 2022; 9(6) doi.org/10.3390/aerospace9060303.
[3] Jiang W, Xie W, Sun S. Parametric optimisation analysis of micro/nano-satellite flywheels based on the NSGA-II optimisation algorithm. Aerospace. 2022; 9(7) doi.org/10.3390/aerospace9070386.
[4] Salmin VV, Kurenkov VI, Safronov SL, et al. Determination of the main design parameters of cost-effective remote sensing satellite systems at the stage of preliminary design. Journal of Physics: Conference Series. 2021; 1745: 012089.
[5] Sedelnikov AV, Khnyryova ES, Ivashova TA. Some features of a small spacecraft application as a technique for the world ocean exploration. IOP Conference Series: Earth and Environmental Science. 2019; 272: 032045.
[6] Sedelnikov AV. Algorithm for restoring information of current from solar panels of a small spacecraft prototype "Aist" with help of normality condition. Journal of Aeronautics, Astronautics, and Aviation, 2022; 54(1): 67-76.
[7] Taneeva AS, Lukyanchik VV, Khnyryova ES. Modeling the dependence of the specific impulse on the temperature of the heater of an electrothermal micro-motor based on the results of its tests. Journal of Physics: Conference Series. 2022; 2096: 012059.
[8] Belousov AI, Sedelnikov AV. Probabilistic estimation of fulfilling favorable conditions to realize the gravity-sensitive processes aboard a space laboratory. Russian Aeronautics. 2013; 56(3): 297-302.
[9] Sedelnikov AV, Potienko KI. Analysis of reduction of controllability of spacecraft during conducting of active control over microaccelerations. International Review of Aerospace Engineering. 2017; 10(3): 160-166.
[10] Kirilin AN. Small spacecrafts of a Aist series (design, tests, operation, development), 1st ed.; Publishing House of the Samara Scientific Center: Samara, Russia. 2017; p. 348.
[11] Dong W, Duan W, Liu W, Zhang Y. Microgravity disturbance analysis on Chinese space laboratory. NPJ Microgravity. 2019; 5(18).
[12] Liu W, Gao Y, Dong W, Li Z. Flight test results of the microgravity active vibration isolation system in China's Tianzhou-1 mission. Microgravity Science and Technology. 2018; 30(6): 995-1009.
[13] Bogatyi AV, Dyakonov GA, Kashirin DA, Popov GA, Semenikhin SA. Development and testing of low-power EP based on the ablative pulsed plasma thruster for an ERS SSC. Journal of Physics: Conference Series. 2021; 1925: 012011.
[14] Hu WR, Zhao JF, Long M, et al. Space program SJ–10 of microgravity research. Microgravity Science and Technology. 2014; 26(3): 159-169.
[15] Yang H, Liu L, Liu Y, Li X. Modeling and micro-vibration control of flexible cable for disturbance-free payload spacecraft. Microgravity Science and Technology. 2021; 33(4): 46.
[16] Sedelnikov AV. Classification of microaccelerations according to methods of their control. Microgravity Science and Technology. 2015; 27(3): 245-251.

[17] Sedelnikov AV, Potienko KI. How to estimate microaccelerations for spacecraft with elliptical orbit. Microgravity Science and Technology. 2016; 28(1): 41-48.
[18] Ovchinnikov MY, Penkov VI Roldugin DS, Ivanov DS. Magnetic navigation systems of small satellites, 1st ed.; Applied Mathematics Institute of M.V. Keldysh of the Russian Academy of Sciences: Moscow, Russia. 2016; p. 366.
[19] Sedelnikov AV, Filippov AS, Gorozhakina AS. Evaluation of calibration accuracy of magnetometer sensors of AIST small spacecraft. Journal of Physics: Conference Series. 2018; 1015: 032045.
[20] Sedelnikov AV, Salmin VV. Modeling the disturbing effect on the AIST small spacecraft based on the measurements data. Scientific Reports, 2022, 12, 1300.
[21] Taneeva AS. The formation of the target function in the design of a small spacecraft for technological purposes. Journal of Physics: Conference Series. 2021; 1901: 012026.
[22] Abrashkin VI, Puzin YY, Filippov AS, Voronov KE, Piyakov AV, Semkin ND, Sazonov VV, Chebukov SY. Uncontrolled attitude motion of the small satellite AIST. Cosmic Research, 2015, 53, 5, 360-373.
[23] Krestina AS, Tkachenko IS. Efficiency assessment of the deorbiting systems for small satellite. Journal of Aeronautics, Astronautics, and Aviation. 2022; 54(2): 227–239.
[24] Semkin ND, Sazonov VV, Voronov KE, Piyakov AV, Dorofeev AS, Ilyin AB, Puzin YY, Vidmanov AS. Magnetic field measurments at small spacecraft "Aist". Physics of Wave Processes and Radio Engineering System. 2015; 18(4): 67-73.
[25] Sedelnikov AV, Filippov AS, Ivashova TA. Earth's magnetic field measurements data accuracy evaluation on board of the small spacecraft "Aist" flight model. Jordan Journal of Mechanical and Industrial Engineering. 2018; 12(4): 253-260.
[26] Semkin ND, Voronov KE, Piyakov AV, Rodin DV, Kalaev MP. A system for compensating microaccelerations of the AIST small spacecraft. Instruments and Experimental Techniques. 2015; 58(4): 562-568.
[27] Sedelnikov AV, Khnyryova ES, Filippov AS, Ivashova TA. Measurements analysis of the earth's magnetic field data obtained from the flight model of AIST small spacecraft. International Journal of Mechanical Engineering and Robotic Research. 2019; 8(4): 542-546.
[28] Avanzini G, Giulietti F. Magnetic detumbling of a rigid spacecraft. Guidance, Control, and Dynamics. 2012; 35(4):1326-1334.
[29] Liu HY, Wang HN, Chen ZM. Detumbling controller and attitude acquisition for micro-satellite based on magnetic torque. Journal of Astronautics. 2007; 28(2): 333-337.
[30] Sedelnikov AV, Orlov DI. Development of control algorithms for the orbital motion of a small technological spacecraft with a shadow portion of the orbit. Microgravity Science and Technology. 2020; 32(5): 941-951.
[31] Skvortsov YV, Evtushenko MA, Khnyryova ES. Investigation of the edge effect in laminated composites using the ANSYS software. Journal of Aeronautics, Astronautics, and Aviation. 2022; 54(4): 421–431.
[32] Sedelnikov AV. Accuracy assessment of microaccelerations simulation on the spacecraft "Foton-M" no. 2 according to magnetic measuring instruments data. Microgravity Science and Technology. 2020; 32(3): 259-264.